Chatter-Free Distributed Control for Multi-agent Nonholonomic Wheeled Mobile Robot

Abdullah Y. Tameem[a]*, Belkacem Kada[b], Ahmed A. Alzubairi[c]

[a,b,c]*Aerospace Engineering Department, King Abdulaziz University, Jeddah 21589, Saudi Arabia*

[a]*Email: atameem0004@stu.kau.edu.sa*
[b]*Email: bkada@kau.edu.sa*
[c]*Email: aalzubairi@stu.kau.edu.sa*

Abstract

This paper proposes to design a chatter-free distributed control for multiagent nonholonomic wheeled mobile robot systems employing terminal exponential functions with graph theory. The terminal tracking criteria are estimated using the Lyapunov approach. The development of distributed control for nonholonomic multiagent wheeled robot systems is defined in the paper along with consensus tracking for undirected fixed/switched topologies. Numerical simulations have been done in order to assess the efficacy and efficiency of the proposed distributed control method in multiple scenarios.

Keywords: Formation Control; Nonholonomic Wheeled Mobile Robot; Multi-agent Systems.

1. Introduction

Control of Multiagent Systems (MAS) has so far been a driving factor in numerous inquiries and evaluations of networks of automated systems like multi-robot, manufacturing manipulators, and Unmanned Aerial Vehicles (UAVs). Extensive studies have presented numerous control protocols to guarantee that MAS can efficiently complete consensus, formation, tracking, and cooperative tasks in various situations [1-6].

In recent decades, Distributed Consensus (DC) of MAS has been used to control nonholonomic Wheeled Mobile Robots (WMR) to provide higher mobility, reliability, adaptivity, resilience, and solidity than single-agent systems [7-13].

----

* Corresponding author.

Tracking geometrical patterns (formation control along desired trajectories) deserves more investigation in multiple nonholonomic WMR cooperative control. Chen and his colleagues [2] offer a unique receding-horizon leader-follower (L-F) controller as a solution to the problem of resolving the formation control of multiple nonholonomic WMR in order to achieve a quick convergence rate of the tracking errors associated with the formation. In order to suppress chattering, Lipschitz approximations make use of the sign function. A distributed cooperative control technique based on local coordinate changes and feedback was proposed by Wang and his colleagues [14]. Park and Yoo [15] investigated obstacle avoidance for performance-based L-F formation control with communication and sensor range restrictions. Lu and his colleagues [16] investigated the distributed L-F formation control of nonholonomic WMR using local communications among individual robots. Kowdiki and his colleagues [17] proposed a framework for formation control in which the robot leader autonomously plans its navigation route in a noisy environment using incrementally path planning by a customized artificial potential environment. This framework was developed for robot formation, where the follower robots will design their paths following the leader robot by applying the separation-bearing l-ψ control to keep a specific formation. Formation control of nonholonomic WMR was investigated by Recker and his colleagues [18], who compared it with two methods that are often applied (a cartesian reference-based controller and a l-ψ controller). Through a series of simulations, studies examined the approaches regarding object transport with various formation geometries. Dong [19] emphasized how vital it is to maintain formation control even when there is a limited amount of tracking information available for agents. Ghasemi and Nersesov [20] employed sliding mode control (SMC) with Euler–Lagrange dynamics for followers to improve the dynamic stability of MAS. Individual agents were provided with decentralized control inputs so that the required formation pattern could be achieved and maintained. Non-smooth sliding surfaces were introduced in this approach to ensure agent fault states descend to the origin in a limited time, hence ensuring finite-time agent coordination. A consensus-based approach was presented by Peng and his colleagues [21] in order to transform and solve the issue of distributed formation control as a state consensus problem. The authors of this approach used adaptive dynamic control systems and distributed kinematic controllers to guarantee that groups of nonholonomic WMR would approach their pattern-optimal states. Distributed state transition observers were used by Yu and his colleagues [22] in order to make a case for a time-varying formation control. Various WMR system formation control techniques were designed by Gamage and his colleagues [23] in order to conduct various experimental implementations.The SMC approach guarantees finite-time convergence and provides robustness against parameter uncertainties and external disturbances in all aforementioned distributed controllers. However, the use of SMC leads to the chattering effect. The results of those studies, which addressed practical problems such as formation accuracy, stability, and noise impact, revealed that when the signum function is employed, the linear and angular velocity profiles cause chattering effects. High-frequency vibrations generated by controller chattering or rapid switching may be hazardous and damaging to the controllers and the whole system [24]. Many studies considered continuous-DC as an alternative to the SMC-based or discontinuous-DC approach by designing enhanced tracking algorithms of a smoothly distributed coordination. Cao and his colleagues [25] devised other alternatives to the discontinuous-DC method proposed by Cao and Ren [1]. This method eliminates the SMC's discontinued element and suggests a continuous component with a feedback gain matrix obtained using the Lyapunov finite-time stability technique. The following are the primary benefits of the continuous-DC outlined in this research: The chattering impact in

discontinuous-DC protocols [4, 26-31] is reduced by using continuous functions that approach zero convergence, and nonlinear functions explain agent behavior rather than linear dynamics or single-integrator as in [25, 32], and the research approach is effectively built to handle patterning track concerns for a group of WMR executing form. The simulation findings reveal superior performance tracking and safe control inputs in comparison to the tracking control proposed by Dong [19] and Peng and his colleagues [21] for multiple robots. However, computing a feedback gain matrix makes the cost of this approach high.This paper offers a unique continuous-distributed consensus control (continuous-DCC) approach for nonlinear MAS. It is characterized as smooth-DCC for nonlinear MAS operating within undirected interaction graphs, as well as fixed/switching topologies. The primary benefits of this continuous-DCC approach are the chattering free control inputs to MAS dynamics and the low number of feedback gains (i.e., only two control gains).The remaining sections of this paper are grouped as follows. Section 2 set up the graph theory's prerequisites and assumptions. Section 3 demonstrates the kinematics WMR system as an agent and within the continuous formation. In section 3, a time-fixed consensus control is proposed for the consensus tracking with fixed undirected interaction topologies and the formation problem, along with their mathematical proofs. Finally, in section 5, The convergence of the state vectors is demonstrated via a numerical simulations model. The paper concluded with a summary of the proposed control feasibility and future work.

2. Preliminaries

Multiagent systems with an several number of followers (ranging from "1" to " n "), as well as a "0" for virtual leader, are used in the following steps. Multi-robot consensus control is established using graph theory to measure the topology of communication between the agents. The communication topology of a group of robots may be shown as the graph $\mathcal{G} = (\mathcal{V}, \mathcal{E}, \mathcal{A})$. The robots (agents) are represented with a set of nodes $\mathcal{V} = (v_1, v_2, \dots, v_n)$, and a set of edges $\mathcal{E} \subseteq \mathcal{V} \times \mathcal{V}$ that indicates the connections between each agent with the other through connectivity weighted adjacency matrix $\mathcal{A} = (a_{ij} \geq 0) \in \mathbb{R}^{n \times n}$ associated with the graph $\mathcal{G}$. Each edge $(ij) \in \mathcal{E}$ determines the flow of the communication where agent i can receive information from the agent j.

Definition 1: Define a matrix M as $M = \mathcal{L} + \mathcal{D}_0$ where $\mathcal{D}_0 = diag(a_{i0})$.

Definition 2: the Graph $\mathcal{G}$, it is defined that the Laplacian matrix $\mathcal{L}$ as $\mathcal{L} = \mathcal{D} - \mathcal{A}$ where $\mathcal{D} = diag(d_i = \sum_{j=1}^{n} a_{ij})$. The node v_0.represents the leader.

Definition 3: The eigenvalues of the Laplacian matrix $\mathcal{L}$ are defined $\lambda_i(\mathcal{L})$ so that $0 \leq \lambda_1(\mathcal{L}) < \lambda_2(\mathcal{L}) < \cdots < \lambda_n(\mathcal{L})$.

Assumption 1: Topology communication is limited to the leader to the followers and does not cover the entire graph $\mathcal{G}$.

3. System Model

3.1. Multiagent nonholonomic wheeled mobile robot kinematics

Consider a multiagent system of n nonholonomic Multiple-Wheeled Mobile Robots (MWMR). Considering the virtual differential Wheel Mobile Robot (WMR), the trajectory of the robots can be estimated, as shown in
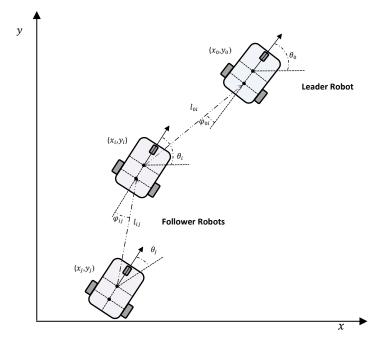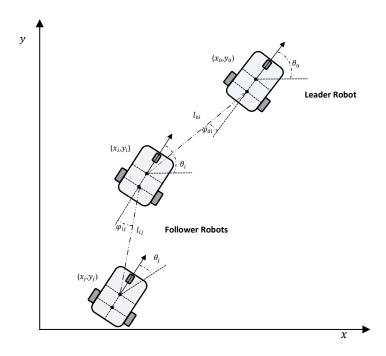
Figure **1**.

Figure 1: Multiagent nonholonomic wheeled mobile robot kinematics

The following equations define a nonholonomic robot agent with nonlinear kinematics:

$$\begin{bmatrix} \dot{x}_i \\ \dot{y}_i \\ \dot{\theta}_i \end{bmatrix} = \begin{bmatrix} cos(\theta_i) & 0 \\ sin(\theta_i) & 0 \\ 0 & 1 \end{bmatrix} \begin{bmatrix} v_i \\ \omega_i \end{bmatrix} \#(1)$$

where x_i, y_i denote the coordinates and θ_i denotes the heading angle of the ith WMR agent, respectively. While v_i and ω_i denote the linear and angular velocity of the ith WMR agent, respectively. The kinematics of each agent 'i' satisfy the following non-slipping time-independent and pure rolling constraints, such that:

$$\dot{y}_i\, cos(\theta_i) - \dot{x}_i\, sin(\theta_i) = 0 \#(2)$$

3.2. The formulation of continuous consensus

The following equation defines the nonlinear dynamics of the followers and the virtual leader.

$$\dot{x}_i = f_i(x_i) + u_i + d_i \#(3)$$

Where, $x_i \in \mathbb{R}^m$, $u_i \in \mathbb{R}^m$, and $d_i \in \mathbb{R}^m$ are the state, control effort, and external disturbances vectors of the ith follower, respectively. $f_i \in \mathbb{R}^m$ defines a set of uncertain nonlinear smooth functions. The leader dynamics are given by:

$$\begin{cases} \dot{x}_0 = f_0(x_0) \\ y_0 = x^{ref} \end{cases} \#(4)$$

where $x_0 \in \mathbb{R}^m$ and $y_0 \in \mathbb{R}^m$ defines the leader's state and output vectors, respectively. x^{ref} denotes the reference state and $f_0 \in \mathbb{R}^m$ is a continuous vector-valued function.

The control objective is to suggested a smooth continuous distributed consensus control input $u_i(x_i)$ for agents $i = 1, \dots, n$ to follow the leader's sates y_0. Furthermore, avoiding chattering due to the heritage of distributed protocols. Following is an agreement that specifies the successful completion of the finite-time consensus local tracking:

Assumption 2: $\forall\, x_i^0 \in D \subset \mathbb{R}^m$ $\exists\, t_s$ (i.e. a settling time) for which

$$\lim_{t \to t_s} \|x_i(t) - x_0(t)\| = 0 \qquad \forall i = 1,2,\dots,n \#(5)$$

4. Main Results

We propose the design of time-fixed consensus control input u_i for the multiagent system considering a fixed topology MAS, in which the followers' state vectors track a dynamic virtual leader state vector.

4.1. Consensus tracking with fixed undirected interaction topologies

Theorem: suppose that assumption 1 holds. The following distributed consensus control asymptotically

guarantees the consensus tracking with directed fixed-time topology:

$$\boldsymbol{u}_i = -\alpha \boldsymbol{e}_i - \beta |\boldsymbol{e}_i|^\gamma \#(6)$$

$$where \begin{cases} e_i = \sum_{j=0}^{n} a_{ij}\left(x_i(t) - x_j(t)\right) \\ \alpha \geq \rho \dfrac{\lambda_{max}(\boldsymbol{M})}{\lambda_{min}^2(\boldsymbol{M})} \\ \beta \geq \dfrac{\sqrt{\tilde{\xi}_0^T(\boldsymbol{M}\otimes\boldsymbol{I}_N)\tilde{\xi}_0}\sqrt{\lambda_{max}(\boldsymbol{M})}}{t_s\lambda_{min}(\boldsymbol{M})N_K}(1+d_0) \\ t_s = \dfrac{\sqrt{\tilde{\xi}_0^T(\boldsymbol{M}\otimes\boldsymbol{I}_N)\tilde{\xi}_0}\sqrt{\lambda_{max}(\boldsymbol{M})}}{\beta\lambda_{min}(\boldsymbol{M})N_K} \end{cases} \#(7)$$

where $N = nm$, $\lambda_{min}(\boldsymbol{M}) > 0$, e_i is a tracking error for each agent $e_i \in \mathbb{R}^m$, m is the system dimension.

Proof: Referring to distributed consensus protocol in (6), consider a tracking error for each agent, that is $\tilde{\xi}_i = \boldsymbol{x}_i - \boldsymbol{x}_0$ $(i = 1, \dots, n)$, then the closed-loop system in (3) and (4) is as follows:

$$\dot{\tilde{\xi}}_i = \boldsymbol{f}_i(\boldsymbol{x}_i) - \boldsymbol{f}_0(\boldsymbol{x}_0) - \alpha \boldsymbol{e}_i - \beta |\boldsymbol{e}_i|^\gamma + \boldsymbol{d}_i(t) \#(8)$$

where α is $diag\,(\alpha_{11}, \alpha_{12}, \cdots, \alpha_{1n})$

For n agents with m states, we rewrite

$$\dot{\tilde{\xi}} = F(\tilde{\xi}, \boldsymbol{x}_0) - \alpha(\boldsymbol{M}\otimes\boldsymbol{I}_N)\tilde{\xi} - \beta\left|(\boldsymbol{M}\otimes\boldsymbol{I}_N)\tilde{\xi}\right|^\gamma + \boldsymbol{D}(t) \#(9)$$

Where:

$$\begin{cases} \tilde{\xi} = \left[\tilde{\xi}_1^T, \dots, \tilde{\xi}_n^T\right]^T \\ F(\tilde{\xi}, \boldsymbol{x_0}) = \left[\left(\boldsymbol{f}_1(\boldsymbol{x_1}) - \boldsymbol{f}_0(\boldsymbol{x_0})\right)^T, \dots \left(\boldsymbol{f}_n(\boldsymbol{x_n}) - \boldsymbol{f}_0(\boldsymbol{x_0})\right)^T\right]^T \\ \boldsymbol{D}(t) = [\boldsymbol{d}_1^T(t), \dots, \boldsymbol{d}_n^T(t)]^T \end{cases}$$

Consider the following Lyapunov candidate function

$$V = \frac{1}{2}\tilde{\xi}^T(\boldsymbol{M}\otimes\boldsymbol{I}_N)\tilde{\xi} \#(10)$$

The derivative of V along the trajectories at (8) is.

$$\dot{V} = \tilde{\xi}^T(\boldsymbol{M}\otimes\boldsymbol{I}_N)\left[F(\tilde{\xi}, \boldsymbol{x}_0) - \alpha(\boldsymbol{M}\otimes\boldsymbol{I}_N)\tilde{\xi} - \beta\left|(\boldsymbol{M}\otimes\boldsymbol{I}_N)\tilde{\xi}\right|^\gamma + \boldsymbol{D}(t)\right] \#(11)$$

$$\dot{V} = \tilde{\xi}^T(M \otimes I_N)F(\tilde{\xi}, x_0) - \alpha\tilde{\xi}^T(M \otimes I_N)^2\tilde{\xi} - \beta\tilde{\xi}^T(M \otimes I_N)\big|(M \otimes I_N)\tilde{\xi}\big|^\gamma + \tilde{\xi}^T(M \otimes I_N)D(t) \#(12)$$

Assumption 3: $\|f_i(x_i)\|_2 \leq \rho\|x_i\|_2$ and $\|f_i(x) - f_i(y)\|_2 \leq \mu\|x - y\|_2$ with $\rho, \mu \in \mathbb{R}^+$.

Lemma 1: A positive-definite symmetric matrix, M, corresponds to a fixed undirected graph, $\mathcal{G}$.

Lemma 2: Li and his colleagues (2011) For a vector $v \in \mathbb{R}^n$ with $1_n^T v = 0$ with $1_n = [1, \cdots, 1]_n^T$, the following inequalities hold $\lambda_{min}(M) > 0$.

$$v^T M v \geq \lambda_{min}(M)v^T v \#(13-1)$$

$$(S \otimes I_N)v \leq \lambda_{max}(S)\|v\|_2 \#(13-2)$$

Considering Assumption 3 and (13-2) results

$$\tilde{\xi}^T(M \otimes I_N)F(\tilde{\xi}, x_0) = F^T(\tilde{\xi}, x_0)(M \otimes I_N)\tilde{\xi} \leq \rho \left\|\tilde{\xi}\right\|_2 \cdot \lambda_{max}(M)\left\|\tilde{\xi}\right\|_2$$

$$F^T(\tilde{\xi}, x_0)(M \otimes I_N)\tilde{\xi} \leq \rho \left\|\tilde{\xi}\right\|_2 \cdot \lambda_{max}(M)\left\|\tilde{\xi}\right\|_2$$

$$\leq \rho \lambda_{max}(M)\left\|\tilde{\xi}\right\|_2^2 \#(14)$$

Considering Assumption (3) and (13-1) results

$$-\tilde{\xi}^T(M \otimes I_N)^2\tilde{\xi} \geq \lambda_{min}^2(M)\tilde{\xi}^T\tilde{\xi}$$

$$\tilde{\xi}^T(M \otimes I_N)^2\tilde{\xi} \leq \lambda_{min}^2(M)\left\|\tilde{\xi}\right\|_2^2 \#(15)$$

Let $g = \big|(M \otimes I_N)\tilde{\xi}\big|^\gamma$

$$-\tilde{\xi}^T(M \otimes I_N)\big|(M \otimes I_N)\tilde{\xi}\big|^\gamma = -\tilde{\xi}^T(M \otimes I_N)g \geq \lambda_{min}(M)\tilde{\xi}^T g$$

$$\tilde{\xi}^T(M \otimes I_N)g \leq \lambda_{min}(M)\left\|\tilde{\xi}\right\|_2\|g\|_2 \#(16)$$

With assumption 3, the derivative (12) is bounded as

$$\dot{V} \leq -\alpha\lambda_{min}^2(M)\left\|\tilde{\xi}\right\|_2^2 - \rho \lambda_{max}(M)\left\|\tilde{\xi}\right\|_2^2 + \beta\lambda_{min}(M)\left\|\tilde{\xi}\right\|_2\|g\|_2 - d_0 \#(17)$$

Assumption 4: There is a function $g \in \mathbb{R}^m$ for each single agent, in order to meet the following conditions

$$\|g\|_2 \leq \|g\|_1 \leq N\|g\|_\infty \leq N_K \#(18)$$

Where $K \in \mathbb{R}^+$

The gains α and β are determined such that $\dot{V} \leq 0 \; \forall t > 0$. Considering assumption 4, this is achieved if and only if

$$\alpha \lambda_{min}^2(\boldsymbol{M}) \left\| \tilde{\boldsymbol{\xi}} \right\|_2^2 - \rho \, \lambda_{max}(\boldsymbol{M}) \left\| \tilde{\boldsymbol{\xi}} \right\|_2^2$$

$$= \left(\alpha - \rho \frac{\lambda_{max}(\boldsymbol{M})}{\lambda_{min}^2(\boldsymbol{M})} \right) \lambda_{min}^2(\boldsymbol{M}) \left\| \tilde{\boldsymbol{\xi}} \right\|_2^2 \geq 0 \#(19)$$

$$\beta \lambda_{min}(\boldsymbol{M}) \left\| \tilde{\boldsymbol{\xi}} \right\|_2 \|\boldsymbol{g}\|_2 - d_0$$

$$= \frac{\beta \lambda_{min}(\boldsymbol{M})\sqrt{2V}}{\sqrt{\lambda_{max}(\boldsymbol{M})}} \|\boldsymbol{g}\|_2 - d_0 \geq 0 \#(20)$$

When $\alpha \geq \rho \frac{\lambda_{\max}(\boldsymbol{M})}{\lambda_{min}^2(\boldsymbol{M})}$, for the undisturbed system $(d_0 = 0)$, $\dot{V}$ will also satisfy

$$\dot{V} \leq - \frac{\beta \lambda_{min}(\boldsymbol{M})\sqrt{2V}}{\sqrt{\lambda_{max}(\boldsymbol{M})}} \|\boldsymbol{g}\|_1 \leq - \frac{\beta \lambda_{min}(\boldsymbol{M})\sqrt{2V}}{\sqrt{\lambda_{max}(\boldsymbol{M})}} N \|\boldsymbol{g}\|_\infty \#(21)$$

$$\sqrt{V} \leq \sqrt{V_0} - \frac{\beta}{\sqrt{2}} \frac{\lambda_{min}(\boldsymbol{M}) \|\boldsymbol{g}\|_\infty}{\sqrt{\lambda_{max}(\boldsymbol{M})}} t \#(22)$$

Taking into consideration assumption 4, the equation (22) results in the settling time is

$$t_s = \frac{\sqrt{\tilde{\boldsymbol{\xi}}_0^T(\boldsymbol{M} \otimes \boldsymbol{I}_N)\tilde{\boldsymbol{\xi}}_0} \sqrt{\lambda_{max}(\boldsymbol{M})}}{\beta \lambda_{min}(\boldsymbol{M}) N_K} \#(23)$$

Regarding the above results, we can finally compute the gains α and β using the following expressions

$$\alpha \geq \rho \frac{\lambda_{max}(\boldsymbol{M})}{\lambda_{min}^2(\boldsymbol{M})} \#(24)$$

$$\beta \geq \frac{\sqrt{\tilde{\boldsymbol{\xi}}_0^T(\boldsymbol{M} \otimes \boldsymbol{I}_N)\tilde{\boldsymbol{\xi}}_0} \sqrt{\lambda_{max}(\boldsymbol{M})}}{t_s \lambda_{min}(\boldsymbol{M}) N_K} (1 + d_0) \#(25)$$

End of the proof.

4.2. Formation problem formulation

Propose the speed control vector $u_i = [v_i \quad \omega_i]^T$ for the ith robot is the primary goal of the multiple robot system into converging into the preferred formation configuration, and the geometric location of the formation and the robots' alignments are intended to converge to the attitude of the virtual leader. (Peng and his colleagues

2016).

$$\dot{\xi}_{1i} = u_{1i}$$

$$\dot{\xi}_{2i} = u_{2i}$$

$$\dot{\xi}_{3i} = u_{1i}\xi_{2i} - k_0|u_{1i}|\xi_{3i} \#(26)$$

where $\boldsymbol{\xi}_i = [\xi_{1i}, \xi_{2i}, \xi_{3i}]^T$ represent the state vector of formation, u_{1i}, u_{2i} are the WMR agent 'i' control inputs and k_0 is a positive constant.

The following equations compute the agents' coordinates

$$x_i = cos(\xi_{1i})\left[\xi_{2i} - k_0 sign(u_{1i})\xi_{3i}\right] + sin(\xi_{1i})\,\xi_{3i} + p_{xi}$$

$$y_i = sin(\xi_{1i})\left[\xi_{2i} - k_0 sign(u_{1i})\xi_{3i}\right] - cos(\xi_{1i})\,\xi_{3i} + p_{yi} \#(27)$$

where p_{xi} and p_{yi} represent the orthogonal coordinates of the WMR agents in the formation pattern F.

Lemma 3: Dong (2012) If $\lim_{t\to\infty}(\xi_{ki} - \xi_{k0}) = 0$ and $\lim_{t\to\infty}(u_{1i} - u_{10}) = 0$ for $(k = 1,2,3)$ and $(1 \leq i \leq n)$, then the multiagent system of n WMRs , for and $(1 \leq i \neq j \leq n)$, the followings hold

$$\lim_{t\to\infty}\begin{bmatrix} x_i - x_j \\ y_i - y_j \end{bmatrix} = \begin{bmatrix} p_{xi} - p_{xj} \\ p_{yi} - p_{yj} \end{bmatrix}, \lim_{t\to\infty}(\xi_{1i} - \xi_{10}) = 0$$

$$\lim_{t\to\infty}\left(\sum_{i=1}^{n}\frac{x_i}{n} - x_0\right) = 0, \lim_{t\to\infty}\left(\sum_{i=1}^{n}\frac{y_i}{n} - y_0\right) = 0 \#(28)$$

where x_0, y_0 denote the leader coordinates and $\xi_{10} = \theta_0$ is its alignment.

Proof: The vector $\tilde{\xi}_{ki} = [(\xi_{k1} - \xi_{10}) \quad (\xi_{2i} - \xi_{20})]^T$ is defined as each WMR agent's tracking error vector. The result of exchanging distributed consensus control (6) for (26) is

$$\dot{\tilde{\xi}}_{1i} - \dot{\xi}_{10} = -\alpha\,\boldsymbol{e}_{1i} - \beta\,|\boldsymbol{e}_{1i}|^\gamma$$

$$\dot{\tilde{\xi}}_{2i} - \dot{\xi}_{20} = -\alpha\boldsymbol{e}_{2i} - \beta|\boldsymbol{e}_{2i}|^\gamma \#(29)$$

where

$$e_{1i} = \sum_{j=1}^{n} a_{ij}\left(\tilde{\xi}_{1i} - \tilde{\xi}_{1j}\right), \;\; e_{2i} = \sum_{j=1}^{n} a_{ij}\left(\tilde{\xi}_{2i} - \tilde{\xi}_{2j}\right)\#(30)$$

Writing the system (29) for n agents, results

$$\dot{\tilde{\boldsymbol{\xi}}} = -\alpha \boldsymbol{M}\tilde{\boldsymbol{\xi}} - \beta \left|\boldsymbol{M}\tilde{\boldsymbol{\xi}}\right|^{\gamma} - \dot{\boldsymbol{\xi}}_0 \#(31)$$

Where $\tilde{\boldsymbol{\xi}} = [\tilde{\xi}_{11}, \tilde{\xi}_{12}, \ldots, \tilde{\xi}_{1n}, \tilde{\xi}_{21}, \ldots, \tilde{\xi}_{2n}]^T$, $\tilde{\boldsymbol{\xi}}_0 = [\tilde{\xi}_{10}\mathbf{1}_n^T, \tilde{\xi}_{10}\mathbf{1}_n^T]^T$, and $\boldsymbol{M}$ is a positive-defined symmetric matrix.

Consider a candidate for the Lyapunov function in order to illustrate the convergence of the formation control (29) as follows:

$$V = \frac{1}{2}\tilde{\boldsymbol{\xi}}^T(\boldsymbol{M} \otimes \boldsymbol{I}_{2n})\tilde{\boldsymbol{\xi}}\#(32)$$

The outcome of substituting the dynamic system error (31) into time derivative (32) is

$$\dot{V} = \tilde{\boldsymbol{\xi}}^T(\boldsymbol{M} \otimes \boldsymbol{I}_{2n})\left[-\alpha(\boldsymbol{M} \otimes \boldsymbol{I}_{2n})\tilde{\boldsymbol{\xi}} - \beta\left|\boldsymbol{M}\tilde{\boldsymbol{\xi}}\right|^{\gamma} - \dot{\boldsymbol{\xi}}_0\right]$$
$$= -\alpha\tilde{\boldsymbol{\xi}}^T(\boldsymbol{M} \otimes \boldsymbol{I}_{2n})^2\tilde{\boldsymbol{\xi}} - \beta\tilde{\boldsymbol{\xi}}^T(\boldsymbol{M} \otimes \boldsymbol{I}_{2n})\left|\boldsymbol{M}\tilde{\boldsymbol{\xi}}\right|^{\gamma} - \tilde{\boldsymbol{\xi}}^T(\boldsymbol{M} \otimes \boldsymbol{I}_{2n})\dot{\boldsymbol{\xi}}_0 \#(33)$$

The demonstration as previous proof results

$$\alpha \geq 0$$

$$\beta \geq \frac{1}{nv}\frac{\sqrt{\tilde{\boldsymbol{\xi}}_0^T(\mathbf{M} \otimes \mathbf{I}_{2n})\tilde{\boldsymbol{\xi}}_0}}{t_s}\frac{\sqrt{\lambda_{max}(\mathbf{M})}}{\lambda_{min}(\mathbf{M})}\#(34)$$

$$t_s = \frac{\sqrt{\tilde{\boldsymbol{\xi}}_0^T(\mathbf{M} \otimes \mathbf{I}_N)\tilde{\boldsymbol{\xi}}_0}}{n(v\beta - \mu)}\frac{\sqrt{\lambda_{max}(\mathbf{M})}}{\lambda_{min}(\mathbf{M})}\#(35)$$

The above examination reaches the convergence $\boldsymbol{\xi}_i \to \boldsymbol{\xi}_0$ with finite time is assured by the input control at (6) under the conditions at (33).

5. Simulations

This section includes a set of simulated scenarios to verify the proposed continuous- DCC and illustrates its effectiveness, primarily with regard to tracking of mobile robots. Consider a team of four mobile robots executing the required geometric pattern illustrated in Figure 2 (a) with fixed-time consensus and undirected switching topology. In the $(\boldsymbol{x}, \boldsymbol{y})$ plane of motion, the pattern of formation may be described, by the orthogonal parameters $(p_{1x}, p_{1y}) = (0, 2)$, $(p_{2x}, p_{2y}) = (2, 0)$, $(p_{3x}, p_{3y}) = (0, -2)$, and $(p_{4x}, p_{4y}) = (-2, 0)$
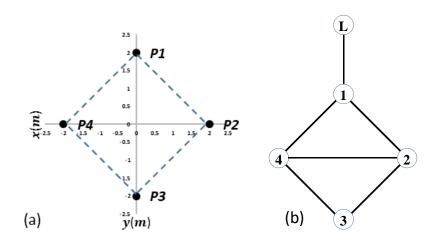
Figure 2: (a) Desired formation pattern (b) Information Exchange

The virtual leader's reference trajectory is determined as $(x_0, y_0, \theta_0) = (0, 12\cos(t/3), t/3)$. The communication graph is presented in Figure 2 (b), where each robot exchanges information with its neighbors based on the distributed structure of the formation control. The continuous-DC control settings are defined as $\tau = 7$, $\alpha = \beta = 3.5$, for u_{1i}, and $\alpha = 0.002$, $\beta = 0.005$ for u_{2i}. Figure 3 shows the fixed-time interaction topology with the consensus interaction graph. In light of the simulation results, the suggested continuous-DC protocol outperforms in terms of fast convergence and smooth control inputs.
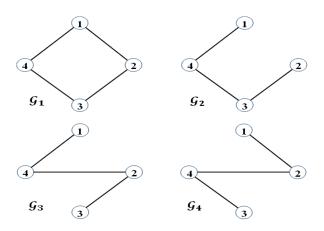

Figure 3: Fixed-time switching topology

Figure 4 illustrates the desired trajectory formation, including the virtual leader centroid and four following robots. The leader robot uses an artificial potential field to lead itself, and the followers successfully follow the leader's path. The leader robot's kinematics control is stable and robust while achieving the objective path, as well as the formation placement and pattern for the time period 0 to 60s. Figure 5 shows the control inputs u_{1i} of the agents, which correspond to different DC protocols which illustrate the agents' state response is shifting while changing topology.
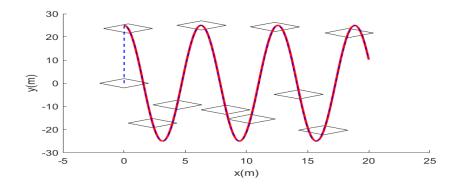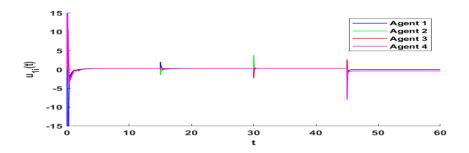
Figure 4: The formation pattern at several moments

Figure 5: Control inputs u_{1i} of the agents

6. Conclusion

The article identifies distributed formation controlling for multiagent nonholonomic wheeled robot systems with consensus tracking for fixed/switched undirected topologies. The leader-follower distributed control technique is used to address the formation of mobile robots. The center point of the formation is considered to be the formation's virtual leader, and the set of mobile robots (followers) tracks the centroid's desired path. The chattering-free distributed protocols developed based on smooth functions have proved their efficiency in maintaining stable formation even when communication between the formation agents is lost. Adaptive control will be used in the future to deal with measurement disturbances, delays, and uncertainty in parameters.

Acknowledgments

References

[1] Y. Cao and W. Ren, "Distributed coordinated tracking with reduced interaction via a variable structure approach," IEEE Transactions on Automatic Control, vol. 57, no. 1, pp. 33-48, 2011.

[2] J. Chen, D. Sun, J. Yang, and H. Chen, "Leader-follower formation control of multiple nonholonomic mobile robots incorporating a receding-horizon scheme," The International Journal of Robotics

Research, vol. 29, no. 6, pp. 727-747, 2010.

[3] R. Olfati-Saber, "Flocking for multiagent dynamic systems: Algorithms and theory," IEEE Transactions on automatic control, vol. 51, no. 3, pp. 401-420, 2006.

[4] W. Ren and R. W. Beard, "Consensus seeking in multiagent systems under dynamically changing interaction topologies," IEEE Transactions on automatic control, vol. 50, no. 5, pp. 655-661, 2005.

[5] Y. Zhao, Z. Duan, G. Wen, and G. Chen, "Distributed finite-time tracking of multiple non-identical second-order nonlinear systems with settling time estimation," Automatica, vol. 64, pp. 86-93, 2016.

[6] L. Cheng, Z.-G. Hou, M. Tan, Y. Lin, and W. Zhang, "Neural-network-based adaptive leader-following control for multiagent systems with uncertainties," IEEE Transactions on Neural Networks, vol. 21, no. 8, pp. 1351-1358, 2010.

[7] X. Li and M. Wang, "Consensus control for wheeled mobile robots under input saturation constraint," IEEE Access, vol. 8, pp. 177125-177130, 2020.

[8] Q. Liu, T. Zhang, H. Li, and Y. Jiang, "Symmetric consensus tracking in nonholonomic mobile multirobot systems," IEEE Access, vol. 9, pp. 43013-43019, 2021.

[9] Z. Wang, L. Wang, H. Zhang, Q. Chen, and J. Liu, "Distributed regular polygon formation control and obstacle avoidance for nonholonomic wheeled mobile robots with directed communication topology," IET Control Theory & Applications, vol. 14, no. 9, pp. 1113-1122, 2020.

[10] J. Mata-Machuca, L. Zarazua, and R. Aguilar-López, "Experimental Verification of the Leader-Follower Formation Control of Two Wheeled Mobile Robots with Obstacle Avoidance," IEEE Latin America Transactions, vol. 19, no. 8, pp. 1417-1424, 2021.

[11] L. Liu, R. Guo, J. Ji, Z. Miao, and J. Zhou, "Practical consensus tracking control of multiple nonholonomic wheeled mobile robots in polar coordinates," International Journal of Robust and Nonlinear Control, vol. 30, no. 10, pp. 3831-3847, 2020.

[12] G. Klančar, D. Matko, and S. Blažič, "Wheeled mobile robots control in a linear platoon," Journal of Intelligent and Robotic Systems, vol. 54, no. 5, pp. 709-731, 2009.

[13] B. Kada, A. S. Balamesh, K. A. Juhany, and I. M. Al-Qadi, "Distributed cooperative control for nonholonomic wheeled mobile robot systems," International Journal of Systems Science, vol. 51, no. 9, pp. 1528-1541, 2020.

[14] G. Wang, C. Wang, Q. Du, L. Li, and W. Dong, "Distributed cooperative control of multiple nonholonomic mobile robots," Journal of Intelligent & Robotic Systems, vol. 83, no. 3, pp. 525-541, 2016.

[15] B. S. Park and S. J. Yoo, "Connectivity-maintaining obstacle avoidance approach for leader-follower formation tracking of uncertain multiple nonholonomic mobile robots," Expert Systems with Applications, vol. 171, p. 114589, 2021.

[16] Q. Lu et al., "Distributed Leader-follower Formation Control of Nonholonomic Mobile Robots," IFAC-PapersOnLine, vol. 52, no. 15, pp. 67-72, 2019.

[17] K. H. Kowdiki, R. K. Barai, and S. Bhattacharya, "Autonomous leader-follower formation control of nonholonomic wheeled mobile robots by incremental path planning and sliding mode augmented tracking control," International Journal of Systems, Control and Communications, vol. 10, no. 3, pp. 191-217, 2019.

[18] T. Recker, M. Heinrich, and A. Raatz, "A Comparison of Different Approaches for Formation Control of Nonholonomic Mobile Robots regarding Object Transport," Procedia CIRP, vol. 96, pp. 248-253, 2021.

[19] W. Dong, "Tracking control of multiple-wheeled mobile robots with limited information of a desired trajectory," IEEE transactions on robotics, vol. 28, no. 1, pp. 262-268, 2012.

[20] M. Ghasemi and S. G. Nersesov, "Finite-time coordination in multiagent systems using sliding mode control approach," Automatica, vol. 50, no. 4, pp. 1209-1216, 2014.

[21] Z. Peng, G. Wen, A. Rahmani, and Y. Yu, "Distributed consensus-based formation control for multiple nonholonomic mobile robots with a specified reference trajectory," International Journal of Systems Science, vol. 46, no. 8, pp. 1447-1457, 2015.

[22] J. Yu, X. Dong, Q. Li, and Z. Ren, "Practical time-varying formation tracking for multiple nonholonomic mobile robot systems based on the distributed extended state observers," IET Control Theory & Applications, vol. 12, no. 12, pp. 1737-1747, 2018.

[23] G. W. Gamage, G. K. Mann, and R. G. Gosine, "Leader follower based formation control strategies for nonholonomic mobile robots: Design, implementation and experimental validation," in Proceedings of the 2010 American control conference, 2010: IEEE, pp. 224-229.

[24] A. Rosales, Y. Shtessel, L. Fridman, and C. B. Panathula, "Chattering analysis of HOSM controlled systems: frequency domain approach," IEEE Transactions on Automatic Control, vol. 62, no. 8, pp. 4109-4115, 2017.

[25] W. Cao, J. Zhang, and W. Ren, "Leader–follower consensus of linear multiagent systems with unknown external disturbances," Systems & Control Letters, vol. 82, pp. 64-70, 2015.

[26] M. Doostmohammadian, "Single-bit consensus with finite-time convergence: Theory and applications,"

IEEE Transactions on Aerospace and Electronic Systems, vol. 56, no. 4, pp. 3332-3338, 2020.

[27] B. Ning, J. Jin, and J. Zheng, "Fixed-time consensus for multiagent systems with discontinuous inherent dynamics over switching topology," International Journal of Systems Science, vol. 48, no. 10, pp. 2023-2032, 2017.

[28] B. Ning, J. Jin, J. Zheng, and Z. Man, "Finite-time and fixed-time leader-following consensus for multiagent systems with discontinuous inherent dynamics," International Journal of Control, vol. 91, no. 6, pp. 1259-1270, 2018.

[29] M. Saim, S. Ghapani, W. Ren, K. Munawar, and U. M. Al-Saggaf, "Distributed average tracking in multiagent coordination: Extensions and experiments," IEEE Systems Journal, vol. 12, no. 3, pp. 2428-2436, 2017.

[30] Z. Zuo and L. Tie, "A new class of finite-time nonlinear consensus protocols for multiagent systems," International Journal of Control, vol. 87, no. 2, pp. 363-370, 2014.

[31] Z. Zuo and L. Tie, "Distributed robust finite-time nonlinear consensus protocols for multiagent systems," International Journal of Systems Science, vol. 47, no. 6, pp. 1366-1375, 2016.

[32] S. Li, H. Du, and X. Lin, "Finite-time consensus algorithm for multiagent systems with double-integrator dynamics," Automatica, vol. 47, no. 8, pp. 1706-1712, 2011.